

# *Numerical simulation of effect of carrier gas on flow state in laser isotope separation*

Jia Ma\*

*China Institute of Atomic Energy, Beijing, 102413, China*

*Jianinajianina@126.com*

*\*Corresponding author*

**Keywords:** Laser isotope separation, Numerical simulation, Supersonic jet flow

**Abstract:** The gas flow in the Condensation Repression by Isotope Selective Laser Activation (CRISLA) is modeled and computed with computational fluid dynamics method. The temperature and velocity distributions of jet flows formed by different gases through nozzle are obtained. Based on the analysis of simulation results, the carrier gas is selected out from the perspective of flow, beneficial to the improvement of isotope separation effect. Our results pave the way towards the follow-up research.

## 1. Introduction

CRISLA is an laser isotope separation (LIS) method, which is expected to be applied in the industrial field<sup>[1]</sup>. Owing to the laser selectivity, the target isotope molecule in the supersonic jet flow is excited, and the laser-excited molecules are inhibited from forming the dimer, while the non-target molecules exist in a form of dimers in the jet flow after colliding with carrier gas. Later, the radial diffusion velocity difference resulting from the mass difference between monomer and dimer leads to the spatial separation of the two. Ascribed to the high selectivity of laser to excite the target isotope molecules, CRISLA has a larger separation coefficient and much lower energy consumption than those of gas diffusion and gas centrifugation with minor mass difference among isotopic molecules.

During the CRISLA process, there would not occur chemical reactions, and moreover, the input state is the same as the output state. Accordingly, the interstage complex processing is avoided for cascade production, as well as the waste pollution is reduced. When separating uranium, U<sub>235</sub> can be almost all recycled, so the depleted tailings from centrifugal plants can be used as feedstock<sup>[2]</sup> to promote the full utilization of uranium resources and reduce radioactive waste.

According to the separation principle of CRISLA, the jet flow should possess the following characteristics to achieve the efficient isotope separation. On the one hand, the jet flow should produce lower temperature. At a lower temperature, the proportion of ground state molecules increases, and the overlap of isotope spectra reduces. This is beneficial to the selective excitation of laser and the formation of dimers. On the other hand, the jet flow should hold a larger diffusion range, conducive to the increase in the spatial separation distance of isotope molecules. Due to the significant influence of supersonic jet flow on CRISLA separation effect, it is a key link to design CRISLA scheme to explore the formation conditions of ideal flow field.

The content of isotope molecules to be separated in the gases with CRISLA is lower, and the physical characteristics of gases mainly refer to those of carrier gas. Thus, different physical characteristics of different gases could result in different temperature and velocity distributions of supersonic jet flow. The previous studies on CRISLA flow field mainly verified and revealed the separation principle of CRISLA from the perspective of flow. Additionally, the studies on carrier gas selection were mainly carried out from the perspectives of spectrum and the formation mechanism of dimer<sup>[3]</sup>. Until now, there are few studies on the analysis of carrier gas selection from the perspective of ideal flow field. The carrier gas, which is more likely to form ideal jet flow, is selected via the analysis of jet flow states from different carrier gases. Such carrier gas can improve the separation effect of CRISLA.

The noble gas has a higher chemical stability, and moreover, their absorption spectra are easily distinguished from those of isotope. Hence, the noble gas is suitable as a CRISLA carrier gas. Herein, the computational fluid dynamics (CFD) software was employed to simulate and compute the jet flow formed by several noble gases, so as to obtain the flow field with a better separation effect of CRISLA. Moreover, the selection of carrier gas was analyzed. Our results can provide a certain reference for the follow-up study on CRISLA.

## 2. Methods and modelling

The STAR-CCM+ software was used for the CFD computation. Moreover, the STAR-CCM+ is a new generation of CFD solver, developed with the computational continuum mechanics algorithms. Hence, STAR-CCM+ is a powerful tool for flow analysis. Firstly, the integral and differential terms in the governing equations of fluid mechanics (Navier-Stokes equation) were approximately expressed in a discrete algebraic form to obtain algebraic equation set. Then, the discrete algebraic equation sets were solved by calculation.

Finally, the numerical solutions of discrete grids were obtained as the approximate solutions of the flow. The Navier-Stokes equation<sup>[4]</sup> of compressible flow illustrates that the change rate of fluid momentum to the time is equal to the resultant force of the external forces exerting on the microelement. Simultaneously, the differential was taken for the Navier-Stokes equation, as follows.

$$\begin{aligned} s_x &= \frac{\partial}{\partial x} \left( \mu \frac{\partial u}{\partial x} \right) + \frac{\partial}{\partial y} \left( \mu \frac{\partial v}{\partial x} \right) + \frac{\partial}{\partial z} \left( \mu \frac{\partial w}{\partial x} \right) + \frac{\partial}{\partial x} (\lambda \cdot \text{div } \mathbf{u}) \\ s_y &= \frac{\partial}{\partial x} \left( \mu \frac{\partial u}{\partial y} \right) + \frac{\partial}{\partial y} \left( \mu \frac{\partial v}{\partial y} \right) + \frac{\partial}{\partial z} \left( \mu \frac{\partial w}{\partial y} \right) + \frac{\partial}{\partial y} (\lambda \cdot \text{div } \mathbf{u}) \\ s_z &= \frac{\partial}{\partial x} \left( \mu \frac{\partial u}{\partial z} \right) + \frac{\partial}{\partial y} \left( \mu \frac{\partial v}{\partial z} \right) + \frac{\partial}{\partial z} \left( \mu \frac{\partial w}{\partial z} \right) + \frac{\partial}{\partial z} (\lambda \cdot \text{div } \mathbf{u}) \end{aligned}$$

Here, the SST k- $\omega$  model<sup>[5]</sup> was used as the turbulence model, and the transport equation is shown as follows.

$$\begin{aligned} \frac{\partial}{\partial t} (\rho k) + \frac{\partial}{\partial x} (\rho k u_x) &= \frac{\partial}{\partial y} \left[ \Gamma_k \frac{\partial k}{\partial y} \right] + G_k - Y_k + S_k \\ \frac{\partial}{\partial t} (\rho \omega) + \frac{\partial}{\partial x} (\rho \omega u_x) &= \frac{\partial}{\partial y} \left[ \Gamma_\omega \frac{\partial \omega}{\partial y} \right] + G_\omega - Y_\omega + D_\omega + S_\omega \end{aligned}$$

Where  $\rho$  is the fluid density.  $\Gamma_k$  and  $\Gamma_\omega$  are the effective diffusion coefficients of  $k$  and  $\omega$ , respectively.  $G_k$  is the turbulent kinetic energy resulting from laminar flow velocity gradient.  $G_\omega$  is from the  $\omega$  equation.  $Y_k$ ,  $Y_\omega$  are the cross-term coefficients of  $k$  and  $\omega$ , respectively.  $D_\omega$  is the orthogonal divergent coefficient.

The computational area of the separation device is shown in Figure 1. In which, ab is the stagnant entry boundary, and the flow direction is perpendicular to the inlet boundary. The bc and cd are the nozzle walls. The de is the vacuum chamber wall, with the adiabatic non-slip wall condition. The ef is the pressure far-field boundary condition. fg is the pressure outlet boundary condition, and ga is the symmetric plane. The boundary temperature and pressure conditions are set in Table 1.

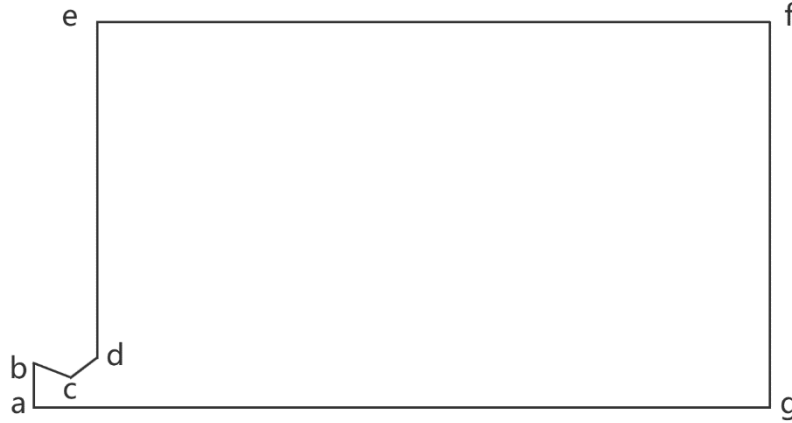


Figure 1. Computational area diagram.

Table 1 Boundary parameters setting.

Boundary	Initial pressure	Initial temperature	Boundary pressure	Boundary temperature
Stagnant entrance ab	1000Pa	300K	1000Pa	/
Pressure exit fg	0.1Pa	300K	0.1Pa	/
Wall bc, cd, de	/	300K	/	/

### 3. Results and Discussion

Because the nozzle structure affects the supersonic jet flow, the nozzle structure should be fixed. The structure parameters are listed in Table 2. The gases are He, Ar and Xe, and their physical parameters are listed in Table 3. Then, the relevant parameters are input into Star-CCM+ software to obtain the jet flow states of different gases through the nozzle.

Table 2 Structure parameters of nozzle.

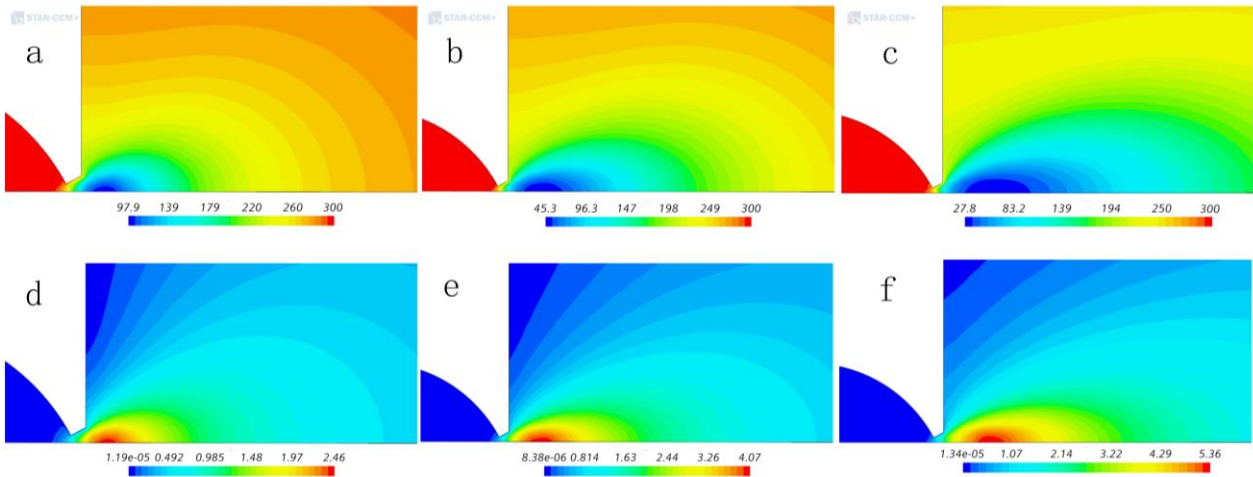
Parameter	Parameter value
Throat diameter of nozzle/mm	2
Expansion length of nozzle/mm	2
Expansion half angle of nozzle/ $^{\circ}$	30

Table 3 Physical parameters of gases.

Physical parameters	He	Ar	Xe
Molecular weight	4.0kg/kmol	39.9kg/kmol	131.3kg/kmol
Dynamic viscosity	2.0E-5Pa-s	2.3E-5Pa-s	2.3E-5Pa-s
Thermal conductivity	0.1549W/m-K	0.0178W/m-K	0.0055W/m-K
Specific heat	5197.61J/kg-K	521.5J/kg-K	158.3J/kg-K

The simulation results of temperature (T/K) distributions and Mach number (Ma) distributions of He, Ar and Xe are shown in Figure 2. It is found that the gas through the nozzle forms the supersonic

jet flow, attributed to the low pressure of vacuum chamber, the underexpanded jet flow continues to expand after entering the vacuum chamber, and the gas temperature decreases. There presents a temperature gradient in the vacuum chamber and forms low-temperature region with the lowest temperature (optimal location for vertical laser irradiation) near the nozzle exit. The temperature and velocity distributions of jet flow formed by different gases are different. The temperature order of three gases in the low-temperature region from low to high is Xe, Ar and He.



a -- He temperature; b -- Ar temperature; c -- Xe temperature; d -- He Mach number; e -- Ar Mach number; f -- Xe Mach number

Figure 2. The flow states of different gases.

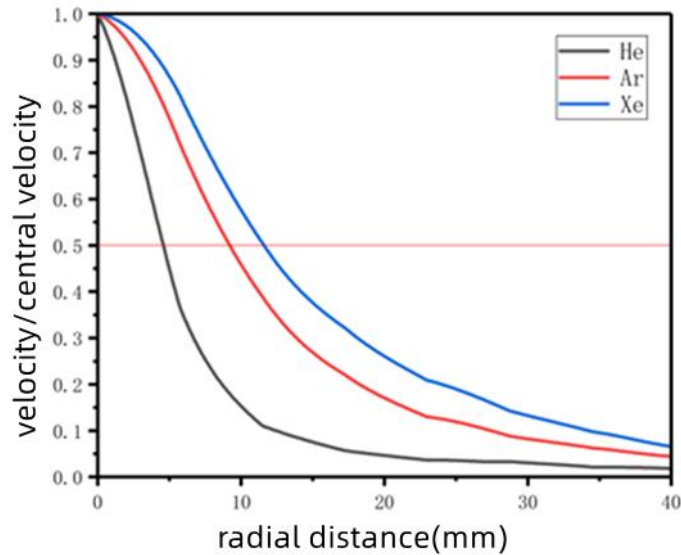


Figure 3. Radial velocity distribution.

The half-value width  $R$  of jet flow can be used to characterize the radial expansion degree of jet flow, defined as the radial distance when the velocity is equal to half of the central velocity. Figure 3 displays the radial velocity distribution in the low temperature region. Notably, the horizontal axis position where the ratio of vertical axis velocity/central velocity is 0.5 is the half-value width of the

jet flow. Obviously, the radial half-value widths  $R(Xe)$ ,  $R(Ar)$  and  $R(He)$  of the three gases in the low-temperature region are 11.49mm, 9.38mm and 4.10mm, respectively. This indicates that Xe's jet flow velocity decays more slowly along the radial direction, thus expanding further in the radial direction. According to the adiabatic expansion relationship, the gas volume expands, and the pressure decreases, resulting in the temperature decrease. This is consistent with the simulation result of lower temperatures caused by Xe gas.

#### 4. Conclusions

The CFD software is used to compute the jet flows of different gases in the CRISLA device. The flow states distribution in device is obtained, and the conclusions are as follows.

(1) Under simulation conditions, the three carrier gases can all form supersonic jet flows, and there appears ideal jet flow in low-temperature region (the optimal region of laser irradiation).

(2) The type of carrier gas significantly affects the temperature distribution and Mach number distribution of jet flow.

(3) It is concluded that Xe is an ideal carrier gas for CRISLA based on the temperature and radial expansion degree of jet flow.

#### References

- [1] Jeff W, Eerkens Jaewoo Kim. *Isotope separation by selective laser-assisted repression of condensation in supersonic free jets [J]. Aiche Journal*, 2010, 56(9):2331-2337
- [2] Wu Haosong, Dai Ding. *U.S. Department of Energy and Global Laser Enrichment Revise Depleted Uranium Supply Agreement[J]. Foreign Nuclear News*, 2020, (07):24.
- [3] Aaron Taylor Baldwin. *Optimization and Analysis of the Laser Isotope Separation Technique SILEX and Ensuing Proliferation Ramifications [D]. Boston: Massachusetts Institute of Technology*, 2016.
- [4] Anderson J D, Wendt J. *Computational fluid dynamics [M]*. New York: McGraw-Hill, 1995.
- [5] Zhao Fei, Zhang Yanling, Zhu Rong, Wang Hui. *Turbulence model in supersonic jet flow field [J]. Chinese Journal of Engineering*, 2014, 36(03):366-372